5th International Biennial Conference on Ultrafine Grained and Nanostructured Materials, UFGNSM15

# Microstructural and Mechanical Properties of Nano/Ultra-Fine Structured 7075 Aluminum Alloy by Accumulative Roll-Bonding Process

H. Alvandi[a,*], K. Farmanesh[a]

[a]*Department of Materials Engineering, Malek -e- Ashtar University of Technology, Isfahan, Iran*

**Abstract**

In this paper, microstructure and mechanical properties of Nano/ultra-fine structured 7075 Aluminum alloy were investigated by accumulative roll bonding process at room temperature. After the accumulative roll bonding, the tensile yield strength, ultimate strength and microhardness of the Nano/ultra-fine structured 7075 Aluminum alloy were 216%, 114%, and 122% higher than those of the coarse-grained samples, respectively, while elongation to failure was lower than the primary sample. The elongation to failure decrease value is high after the first pass while after subsequent passes, it remains almost constant. Evolution of microstructure of the samples was investigated by transmission electron microscopy (TEM) and field emission scanning electron microscope (FESEM). In addition, phase analysis after ARB were performed using X-ray diffraction analysis. The micro scale tensile fracture morphology of the Al 7075 alloy at different ARB strains were investigated by using FESEM. According to TEM micrographs, the ARB processed materials after six passes were homogeneously filled with the ultra-fine grains, meaning that grain sizes were about 130 nm. XRD, FESEM and TEM results show that $MgZn_2$ precipitates were broken, and small spherical particles were formed during ARB, which is distributed uniformly throughout the material. Uniform distribution of these fine particles restricted grain growth, resulting in the formation of ultra-fine grains. Fracture morphologies of samples after ARB show that the average dimple size gradually decreases with increasing number of ARB passes, which lead to fracture type changes from ductile to brittle.

* Corresponding author. Tel.: +989129314389.
*E-mail address:* Hossein_Alvandy@yahoo.com

## 1. Introduction

Severe plastic deformation (SPD) is a reliable method for grain refinement in metals and alloys. Ultrafine grained (UFG) metals and alloys processed by severe plastic deformation (SPD) techniques have been reported to have superior mechanical properties, such as high strength and hardness with good ductility and excellent superplasticity at lower temperature and higher strain, Anghelus et al (2015), Chen et al (2006), Karlık et al (2004), Koizumi et al (2003). Among all the SPD techniques, accumulative roll bonding (ARB), developed by Saito et al (1998), is especially attractive because it can produce large bulk semi-products using a conventional rolling mill. This method has some advantages over other SPD processes. There is no need to form facilities with large load capacities and expensive dies; furthermore, production rates can be high, and the amount of material to be produced is not limited, Saito et al (1998), Eizadjou et al (2012). According to this process, a sheet of material is rolled to 50% reduction and then it is cut into two portions, which are stacked together and rolled again. This procedure can be repeated many times so as to achieve the final total strain required. The ARB technique does not require any special equipment and can be used to apply very large strains as the initial dimensions of the sample do not change, Iwahashi et al (1996), Saito et al (1999), Valiev (2004), Xu et al (2003), Zhao et al (2004). The ARB process has been widely and successfully performed on pure aluminum and different aluminum alloys such as AA6061, Lee et al (2002), AA3003, Xing et al (2002), AA8006, Xing et al (2002), AA5086, Roy et al (2011) and A356, Jamaati et al (2011). However, low attention has been paid to 7075 aluminum alloy, Hidalgo et al (2010), Hidalgo et al (2012), which is widely used for high strength structural applications such as automotive, aerospace, military, sports and electronic industries. Cold working, which usually improves the strength of metals and alloys, has been found to be ineffective in improving the strength of 7000 series of Al alloys, Huang et al (2003). The 7075 aluminum alloy plate, in O temper condition, has practical and industrial applications due to its higher formability in comparison to other temper conditions. In the present investigation, a commercial 7075 Al alloy was severely processed by ARB. Al 7075 (annealed at 413℃) was ARBed at room temperature to six passes. The microstructural and mechanical properties in Al 7075 alloy after ARB are discussed below.

## 2. Experimental procedure

The material used in this study was a 7075 aluminum alloy sheet of the chemical composition presented in table 1. The starting material showed a fully annealed microstructure filled with equiaxed grains with the mean grain size of 36µm. The field emission scanning electron microscope (FESEM) micrograph of longitudinal cross-section of initial sheet is shown in Fig. 1a. To achieve a good bonding, the surfaces of the two sheets with dimensions of 200 mm×50 mm×1 mm were degreased (in acetone) and wire brushed (with a stainless steel brush with wires of 0.4 mm in diameter).

Table 1. Chemical composition of Al 7075 alloy.

| Element | Zn | Cu | Mn | Mg | Cr | Si | Fe | Ti | Other | Al |
|---|---|---|---|---|---|---|---|---|---|---|
| Content wt-% | 5.5 | 1.5 | 0.3 | 2.5 | 0.19 | 0.4 | 0.5 | 0.1 | 0.15 | reminded |

Two sheets were stacked and bound tightly. The stacked sheets were then rolled to 50% reduction in thickness. The roll bonded sheet was cut in half and stacked to the initial thickness. The stacked sheets were rolled again with the same reduction ratio and the same procedure was repeated up to six cycles (the total equivalent strain was 4.8) at ambient temperature. Samples were taken after first, third and sixth cycles of ARB for testing. Rolling was performed in non-lubricated conditions by using two mills with a roll diameter of 145 mm, and the roll peripheral speed was 4.1 m min-1. Afterwards, it was divided into two identical pieces that were supplied to the next ARB pass. The microstructure of the ARBed samples was examined by FESEM and transmission electron microscopy (TEM). The FESEM studies were carried out in a Mira 3-XMU FESEM equipped with Energy Dispersive x-ray spectroscopy (EDS) operating at 20kV with a working distance of 15mm. The TEM study was conducted with a JEOL JEM 2000 FX II microscope operating at 200 kV. The mean grain size of the ARBed samples was calculated from TEM micrographs. For the TEM investigation, a thin rectangular foil, perpendicular to the transverse direction, was prepared

by twinjet polishing technique using a solution of 400 ml HNO3and 800 ml CH4OH. X-ray diffraction patterns were used to identify the presence of different phases in the starting material and the ARBed samples. A Philips diffractometer (40 kV) with Cu Kα radiation ($\lambda = 0.15406$ nm) was used for XRD measurements. The XRD patterns were recorded in the $2\theta$ range of 20–100° (step size 0.03°, time per step 1 s). Vickers microhardness and tensile test were conducted to evaluate the mechanical properties of ARBed samples. Using a load of 15 g for 15 s, Vickers microhardness test was performed on rolling plane (RD–TD plane) of the ARB-processed samples. Mean value of ten separated measurements taken at randomly selected points was reported. The tensile test was carried out using tensometer under constant cross head speed. The sample preparations were carried out as per ASTM E8 standard in order to conduct the tensile test.

## 3. Results and discussions

### 3.1. Microstructure analysis

In Fig. 1, the FESEM micrographs of starting material are illustrated. According to Figs. 1a, b in the annealed condition, a large number of precipitates were distributed heterogeneously throughout the material and lying both within the grain and on the grain boundaries. Careful inspection over a wide area in Fig. 1a showed that the average grain size in this condition was 36μm.
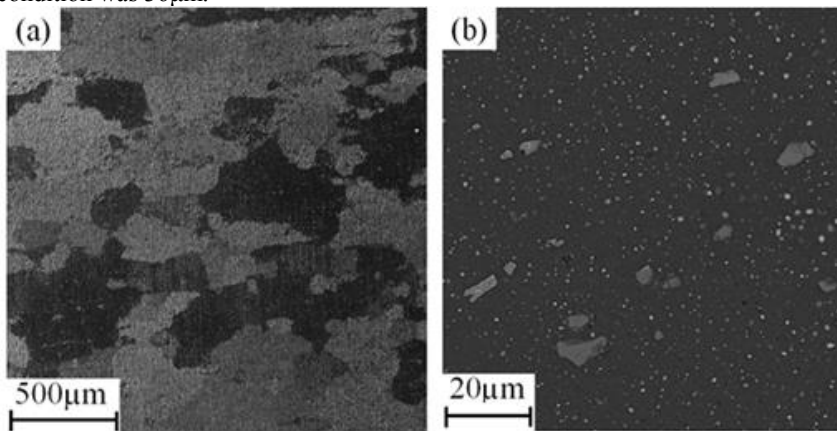


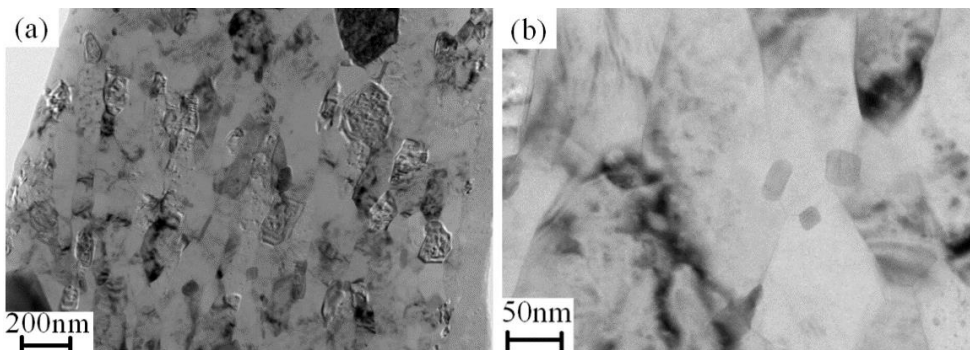Fig. 1. (a) Secondary electron; (b) back scattered electron micrograph of starting material.



Fig. 2. TEM microstructures observed at the TD plane of the specimen ARBed by six cycles.

Figure 2 shows TEM micrographs observed at the TD plane of the ARB processed sheets by six cycles. As shown in Fig. 2, the microstructural characteristics of the material, severely deformed by the ARB process, are similar to those reported in the previous studies. The ultrafine grains elongated along the rolling direction (RD) were homogeneously observed through the large area in the thin foil. It is expected that the ARB processed materials have a complicated change in microstructure through thickness due to the redundant shear strain introduced during roll-bonding. After six cycles, the specimen was filled with ultra-fine grains with average grain size of 130 nm homogenously distributed.
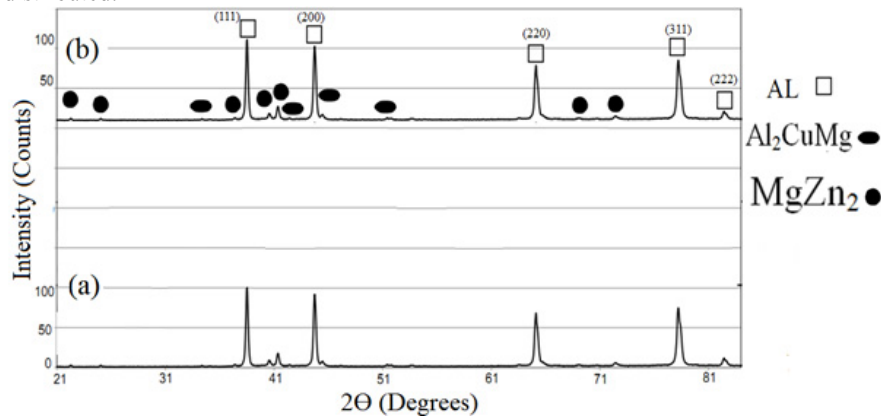


Fig. 3. The X-ray pattern of the 7075 aluminium alloy at different strains (ε); (a) Starting material; (b) ε= 4.8.

Phases were identified using XRD analysis of 7075 Al alloy before and after ARB for six passes shown in Fig. 3. After six passes, very high intensity was obtained from Al. Intensity of MgZn2 decreased after ARB due to very high strain induced and because of fragmentation of precipitates (Fig. 3). In earlier studies on pure and 7075 aluminum alloys, the same observation was noticed after one pass of ARB. The rod shaped MgZn2 precipitates are fragmented and they become spherical with the size of the precipitates in the range of 30–100 nm, Valiev (2004). The same results were seen in Fig. 2b.

### 3.2. Analysis of mechanical properties

Figure 4 shows tensile engineering stress–strain curves of 7075 Al alloy sheets after various cycles of ARB at room temperature. As can be seen, the tensile strength increased strongly after the first cycle of rolling. Of course, this increase was observed with the second cycle. But the tensile strength increases in the third, fourth and fifth cycles are less than those in the first and second cycles. According to previous studies, this is because of dynamic recovery in the higher cycles. The existence of work hardening is attributed to an increase in the dislocation density, the grain refinement and fragmented precipitates. The tensile strength is about 213 MPa for starting material before accumulative roll bonding while it obtains 305 MPa for the rolled sample after one pass. In the third pass, this value reaches 427 MPa. After the fourth pass, the tensile strength is 435 MPa and after the fifth pass, it reaches 470 Mpa, which is twice as much as the starting material. As we will see in the stress-strain curve (Fig. 4), the fracture strain rolled samples are significantly fewer than the fracture strain of starting material and are from about 16.8% to 6.8% percent, and this decrease was reduced to 5%. Increase in the strength for the initial cycles due to work hardening is induced to the increase in the dislocation density. Increase in the strength at higher cycles is possibly due to changes in grain structure.
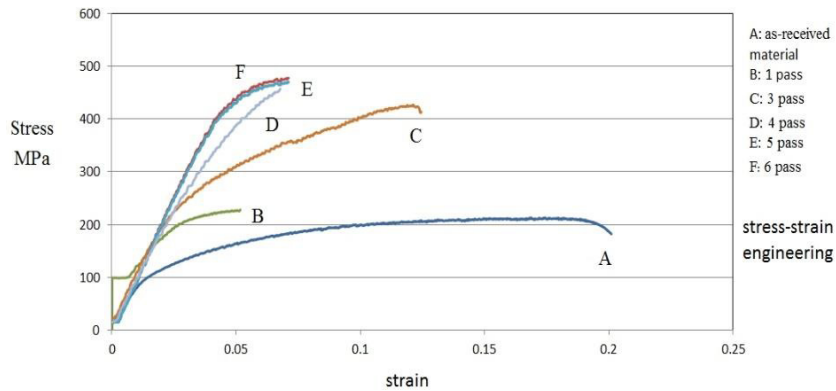
Fig. 4. Engineering stress-strain curves for 7075 aluminium sheet ARB processed.

The reason for the decrease in the strength at cycle six (Strain 8.4) is the recrystallization of the structure. On the other hand, the occurrence of recrystallization caused a reduction in the dislocation density during the accumulative roll bonding process and then, it prevents more strength. Fig. 5 shows the respective variations of hardness values with respect to ARB passes. According to Fig. 5, the trend of microhardness changes of the studied material with respect to ARB passes is the same as that of yield strength changes with ARB cycles. This fact shows that there exists a correlation between yield stress and microhardness in the ARB processed materials similar to those usually observed in the conventionally processed materials. The increase in hardness is due to the fragmentation of the precipitates, increase in the dislocation density and grain refinement according to the Hall–Petch equation (1), where k is the Hall-Petch parameter, H0 is starting material hardness and D is the grain size. The micro hardness has increased from 57 HV to 127 HV after six ARB passes.
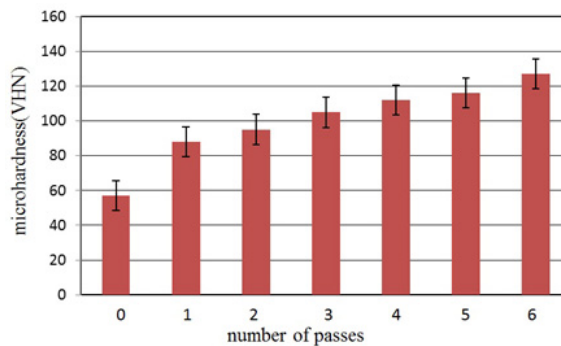
$$H = H_0 + KD^{-\frac{1}{2}} \tag{1}$$



Fig. 5. Variations of Hardness values with number of ARB passes.

### 3.3. Deformation and fracture morphologies

Figure 6 shows the fracture surfaces after tensile tests of the annealed and ARBed specimens at the first, third, and sixth cycles. They reveal that the annealed sample exhibits a typical ductile fracture showing deep equiaxed dimples (Fig. 6a). Clearly, after ARB process, the samples also show a ductile fracture having dimples, but these dimples are not as deep as those in the initial material. Fig. 6b-d shows that by increasing the number of cycles in the ARBed specimens, the equiaxed dimples become finer in size and shallower. As mentioned before, increasing the number of

cycles decreased elongation values in ARBed specimens. Therefore, by increasing the number of cycles, the plastic deformation decreased until fracture and the size and deepness of dimples were reduced. According to previous researchers, the decrease in the dimple size is due to grain refinement as well as work hardening and fragmentation of the particles, Fang et al. (2007).
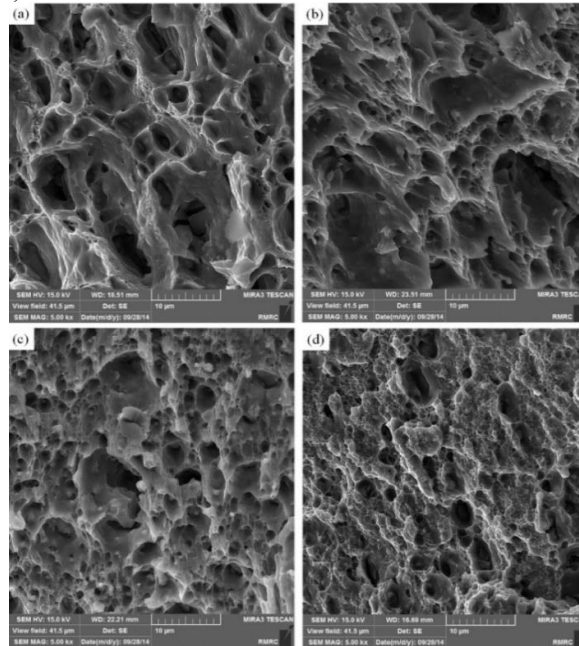


Fig. 6. Tensile fracture surface morphology of annealed condition and accumulative rolled bonding (ARB) Al 7075 alloy samples at different strains (ε); (a) Starting material; (b) ε= 0.8; (c) ε= 2.4 and (d)ε= 4.8.

## 4. Conclusions

In this study, the microstructure and mechanical properties of a 7075 aluminum alloy severely deformed by the ARB process up to 6 cycles were investigated. The main results are summarized as follows:

- UFG microstructures were formed in the 7075 aluminum alloy highly deformed by the ARB process.
- The tensile strength of the ARB processed 7075 Al alloy increases with the number of ARB cycles so that the specimen after five cycles, shows UTS of 470 MPa, which is about three times as much as that in the annealed state. The hardness of the ARB processed 7075 Al increased with the number of ARB cycles so that the specimen after eight cycles achieved the highest hardness of about 112% higher than the initial value.
- Fracture morphology shows a ductile fracture even after ARB. However, the amounts of micro voids are less. In addition, due to fine grains, fine shear lips are observed. Therefore, at higher strains of 2.4 and 4.8, the macrographs clearly indicate the absence of necking and the presence of shear feature.

# References

Anghelus, A., M.-N. Avettand-Fènoël, C. Cordier, and R. Taillard, 2015. Microstructural evolution of aluminium/Al–Ni–Sm glass forming alloy laminates obtained by Controlled Accumulative Roll Bonding. Journal of Alloys and Compounds 631: 209-218.

Chen, M., H. Hsieh, and W. Wu, 2006. The evolution of microstructures and mechanical properties during accumulative roll bonding of Al/Mg composite. Journal of alloys and compounds 416(1), 169-172.

Eizadjou, M., H. Fattahi, A. Talachi, H. Manesh, K. Janghorban, and M. Shariat, 2012. Pitting corrosion susceptibility of ultrafine grains commercially pure aluminium produced by accumulative roll bonding process. Corrosion Engineering, Science and Technology, 47(1): 19-24.

Fang, D., Q. Duan, N. Zhao, J. Li, S. Wu, and Z. Zhang, 2007. Tensile properties and fracture mechanism of Al–Mg alloy subjected to equal channel angular pressing. Materials Science and Engineering: A 459(1), 137-144.

Hidalgo, P., C. Cepeda-Jiménez, O.A. Ruano, and F. Carreño, 2010. Influence of the processing temperature on the microstructure, texture, and hardness of the 7075 aluminum alloy fabricated by accumulative roll bonding. Metallurgical and Materials Transactions A 41(3), 758-767.

Hidalgo-Manrique, P., C. Cepeda-Jiménez, O.A. Ruano, and F. Carreño, 2012. Effect of warm accumulative roll bonding on the evolution of microstructure, texture and creep properties in the 7075 aluminium alloy. Materials Science and Engineering: A 556: 287-294.

Huang, X., N. Tsuji, N. Hansen, and Y. Minamino, 2003. Microstructural evolution during accumulative roll-bonding of commercial purity aluminum, Materials Science and Engineering: A 340(1), 265-271.

Iwahashi, Y., J. Wang, Z. Horita, M. Nemoto, and T.G. Langdon, 1996. Principle of equal-channel angular pressing for the processing of ultra-fine grained materials. Scripta Materialia 35(2), 143-146.

Jamaati, R., S. Amirkhanlou, M.R. Toroghinejad, and B. Niroumand, 2011. Significant improvement of semi-solid microstructure and mechanical properties of A356 alloy by ARB process. Materials Science and Engineering: A 528(6), 2495-2501.

Karlık, M., P. Homola, and M. Slámová, 2004. Accumulative roll-bonding: first experience with a twin-roll cast AA8006 alloy. Journal of alloys and compounds 378(1), 322-325.

Koizumi, Y., M. Ueyama, N. Tsuji, Y. Minamino, and K.i. Ota, 2003. High damping capacity of ultra-fine grained aluminum produced by accumulative roll bonding. Journal of alloys and compounds 355(1), 47-51.

Lee, S., Y. Saito, N. Tsuji, H. Utsunomiya, and T. Sakai, 2002. Role of shear strain in ultragrain refinement by accumulative roll-bonding (ARB) process. Scripta Materialia 46(4), 281-285.

Lee, S., Y. Saito, T. Sakai, and H. Utsunomiya, 2002. Microstructures and mechanical properties of 6061 aluminum alloy processed by accumulative roll-bonding. Materials Science and Engineering: A 325(1), 228-235.

Roy, S., S. Singh, S. Suwas, S. Kumar, and K. Chattopadhyay, 2011. Microstructure and texture evolution during accumulative roll bonding of aluminium alloy AA5086. Materials Science and Engineering: A 528(29), 8469-8478.

Saito, Y., N. Tsuji, H. Utsunomiya, T. Sakai, and R. Hong, 1998. Ultra-fine grained bulk aluminum produced by accumulative roll-bonding (ARB) process. Scripta materialia 39(9), 1221-1227.

Saito, Y., H. Utsunomiya, N. Tsuji, and T. Sakai, 1999. Novel ultra-high straining process for bulk materials—development of the accumulative roll-bonding (ARB) process. Acta materialia 47(2), 579-583.

Valiev, R., 2004. Nanostructuring of metals by severe plastic deformation for advanced properties, Nature materials 3(8), 511-516.

Xing, Z., S. Kang, and H. Kim, 2002. Structure and properties of AA3003 alloy produced by accumulative roll bonding process, Journal of materials science 37(4), 717-722.

Xu, C., M. Furukawa, Z. Horita, and T.G. Langdon, 2003. Achieving a superplastic forming capability through severe plastic deformation. Advanced Engineering Materials 5(5), 359-364.

Zhao, Y., X. Liao, Z. Jin, R. Valiev, Y. Zhu, 2004. Microstructures and mechanical properties of ultrafine grained 7075 Al alloy processed by ECAP and their evolutions during annealing. Acta Materialia 52(15), 4589-4599.